

Bi-self-trapping of excitons via the long-living phonon mode and their superfluorescent markers.

Vladimir Al. Osipov

*Institute for Advanced Study in Mathematics, Harbin Institute of Technology,
92 West Da Zhi Street, Harbin, 150001, China and*

*Suzhou Research Institute, Harbin Institute of Technology,
500 South Guandu Road, Suzhou, 215104, China*

Email: Vladimir.Al.Osipov@gmail.com

(Dated: January 29, 2025)

Understanding the origin of the system response offers guidance for designing single-component material devices with required properties. A notable phenomenon of room-temperature superfluorescence recently observed in hybrid perovskites at high concentrations of excitations lacks of comprehensive theoretical framework. Addressing this gap necessitates a discussion grounded in non-linear and multiparticle theories. In this study, we offer the two-step mechanism: formation of two self-trapped excitons entangled via the same long-living phonon mode, and their rearrangement into a superradiating mirror symmetric configuration. Based on the semiclassical equations of motion we examine the criteria for the high-temperature self-trapping and bi-self trapping of excitons. Our findings indicate that the self-trapped excitons are described by the stable phase-locked steady-state solution of the equations of motion, and at elevated exciton concentrations, they compete with the bi-self-trapped excitons. The latter is described by the Dicke model and is thus responsible for the generation of the superfluorescent spectral peak. The obtained theoretical spectra are in good agreement with the experimental observation.

I. INTRODUCTION

The rapid progress in quantum technologies is a source of discovering new complex quantum effects, often requiring the attraction of nonlinear and many-particle concepts. The non-linear theories are known to be important in the theory of polaron [1] and bi-polaron [2], the fermionic quasiparticle composed of a charge carrier “dressed” with the carrier induced lattice polarization. The non-linear terms describe this loop of interactions in the equations of polaron motion. While the polaron theory was originally developed for electrons, there is much experimental and theoretical evidence that neutral bosonic excitons (below we consider only long-ranged Wannier-Mott excitons) form the self-trapped excitons (STE) [3–6], whose formation mechanism is similar to the polaronic one.

The exciton self-trapping was observed in various systems, such as condensed rare gases [7], organic molecular systems [8, 9] and halide systems (see review [5]). Since 2001, when the first report of STEs in the lead halide perovskites at temperatures below 175K was published [10], the broad STE emission was observed in various halide compounds and also at room temperatures [11, 12], which holds a great potential for the white light-emitting single-material diodes [6]. In 2022 a phenomenon of superfluorescence (collective emission of fluorescent light by an ensemble of excited atoms or ions [13]) has been discovered in methylammonium lead iodide beyond 78K [14] and in phenethylammonium caesium lead bromide at room-temperature [15].

The superfluorescence effect is manifested by the appearance of a sharp spectral peak (at 2.36eV) when the intensity of the pumping light (100fs pulses) ex-

ceeds a certain critical value ($25.0\mu Jcm^{-2}$ at 300K and $4.0\mu Jcm^{-2}$ at 78K). The peak appears with a delay of about 10ps (15ps at 78K) against the background of a broad (of 0.15eV width) Gaussian fluorescence peak centered at 2.40 eV. In the original works [14, 15] the effect was explained by a phase transition to a long-range polarons macroscopic coherence mediated by the long-living phonon mode (LLPM). Indeed, the Raman [16] and terahertz [17–19] spectroscopic experiments, and the photoluminescence measurements [20] of the composite organic-inorganic materials reveal the presence of mixed organic-inorganic long-living (decay rates 4 – 6 times smaller than the phonon frequency [19]) longitudinal optical phonon modes (LLPM) with the frequencies ranging from $91cm^{-1}$ to $225cm^{-1}$ ($\sim 10 \div 4 \times 10^5 \text{Å}$) for various materials. The modes are strongly coupled to charge carriers [19, 21], and the coupling constant is of order 2 (for comparison in GaAs it has the value 0.068 [22]). The DFT modelling of hybrid perovskites demonstrated [23] that such type of waves propagates by periodic alternating distortion of organic and inorganic units, which, in turn, causes periodic charge transfer from the organic molecular orbitals to the inorganic electron bands. In this article, we suggest a more preferable two-stage bi-STE formation mechanism leading to the superfluorescence. It includes the stage of bi-STE’ formation due to interaction of two excitons with the same LLPM and the stage of bi-STE’ rearrangement into a (super-)symmetric configuration. The leading terms of the symmetric bi-STE’ subsystem Hamiltonian coincide with the Dicke Hamiltonian (eq. 8), known to describe the superradiance phenomenon [24–27].

Our consideration is based on five observations. (i) The interaction amplitude between a charge and longi-

tudinal optical phonons in polar crystals is described by Frölich amplitude [28–30], which is known to increase for small momenta q . The latter means that when a significant number of phonons is excited, the thermalization process dominates and can destroy any long-range coherences between the carriers [30]. On the contrary, the Frölich type interaction for neutral excitons nullifies at $q = 0$ and reaches maximum at some wavevector [29, 31], which we denote as k_0 . Its value can be estimated from analytic expression to give $a_0 k_0 = \text{const.} \frac{m_e^* + m_h^*}{m_h^*}$, where a_0 is the exciton Bohr radius and the constant is close to 2 (see fig. 1a). The electron and hole effective masses (m_e^* and m_h^*) in perovskites has close values ($m_e^* \sim m_h^*$ and ~ 0.15 of the electron mass [32]), so that k_0 changes in the range 5 to $8 a_0^{-1}$. (ii) The thermalized surrounding of a moving quantum wave packet slows its motion and stabilizes its extension in space [33, 34]. In the presence of the non-linear terms, the initial Gaussian shape packet is deformed, and the formation of the soliton-like solutions becomes possible [35–38]. This means that in the momentum space, the distribution is heavy-tailed (fig. 1b). Combining (i) and (ii) we arrive at the picture when the vector \mathbf{k}_0 fits inside the wave packet at least once. Moreover, considering that the non-linear terms in the equations of motion become important for significant amplitudes only, we simplify our theoretical description and replace the whole exciton packet in the \mathbf{q} -space with only two quantum states connected by the vector \mathbf{k}_0 , the states a and b in fig. 1c and assume that the most of the quantum density is distributed over these two quantum states. (iii) Our semiclassical approach shows that the system of two quantum states shared by one exciton and interacting with LLPM evolves towards a stable phase-locked stationary solution, which we interpret as STE', realising the energy minimum. The STE' solution exists for geometries with arbitrary mutual orientations of the vectors \mathbf{k}_0 , and \mathbf{q}_a (fig. 1c). The non-collinearity causes angular slip of the wave packet in the momentum space until the configuration $\mathbf{k}_0 \parallel \mathbf{q}_a$ is reached. As will be demonstrated, the latter configuration corresponds to the lowest STE' energy. (iv) At high excitation concentrations, *two* excitons may become entangled with the same LLPM. We demonstrate that equations of motion for such two-exciton and one-phonon subsystem possess the stable stationary solution, which we interpret as bi-STE'. The bi-STE' lowest energy is realized for the mirror-symmetric bi-STE' (super-symmetric) configurations (fig. 1e). (v) The excitons are compound particles made of two fermions and thus the operator of exciton creation/annihilation in the quantum state marked by the wavevector \mathbf{q} (\hat{B}_q^\dagger and \hat{B}_q) satisfy the Boson statistics (cobosons [39]). At high temperatures (much higher than the condensation temperature) the probability of the existence of the exciton quantum states with the occupation numbers larger than one tends to zero [3]. Technically, this means that the operators $\hat{B}_q, \hat{B}_q^\dagger$ stay bosons for different \mathbf{q} , while becoming fermions for the same \mathbf{q}

and the multi-excitonic wavefunction in this approximation can contain operators \hat{B}_q^\dagger in the first power only (eq. 2). Such mutual effective repulsion prevents packets from passing through each other and can lead to forming a fermionic condensate (fig. 1d) at high concentrations of excitations. This, in particular, helps in the transition to the supersymmetric configurations, which are the source of superfluorescence.

II. THE SEMICLASSICAL EQUATIONS OF MOTION.

In what follows we consider the system of one and two bright (the total spin is one) s -excitons (the lowest eigenenergy) in the presence of a single LLPM. Within the effective mass approximation the system of Wannier excitons interacting with phonons (boson operators $\hat{b}_\mathbf{k}^\dagger, \hat{b}_\mathbf{k}$) is typically described by the Holstein Hamiltonian [3, 40] (\hbar is set to 1 along the article): b

$$\hat{\mathcal{H}} = \omega_{ph} \sum_{\mathbf{q}} \hat{b}_\mathbf{q}^\dagger \hat{b}_\mathbf{q} + \sum_{\mathbf{q}} W_q \hat{B}_\mathbf{q}^\dagger \hat{B}_\mathbf{q} + \sum_{\mathbf{k}, \mathbf{q}} D(\mathbf{k}) \hat{B}_\mathbf{q}^\dagger \hat{B}_{\mathbf{q}-\mathbf{k}} (\hat{b}_{-\mathbf{k}}^\dagger + \hat{b}_\mathbf{k}) + \hat{\mathcal{H}}_{bath} + \hat{\mathcal{H}}'. \quad (1)$$

The LO phonon frequency ω_{ph} is taken to be \mathbf{q} -independent, and the exciton energy $W_q = E_g + q^2/2M_{ex}$ is composed from the ground state eigenenergy E_g and quadratic in \mathbf{q} kinetic term [29, 41], (the band gap in the vicinity of the Γ -point is direct and almost isotropic [42], so that the exciton mass M_{ex} is a scalar). The last (third) term (eq. 1) stands for phonon-exciton scattering with conservation of the quasi-momentum [29, 43], where $D(-\mathbf{k}) = D^*(\mathbf{k})$ corresponds to the Frölich type of interaction. The $\hat{\mathcal{H}}_{bath}$ term includes interaction of the phonon modes with bath and $\hat{\mathcal{H}}'$ describes the exciton-phonon interaction.

To explore the dynamics of the exciton-phonon system we make use of the multiconfiguration Hartree approach [44–47], known to be useful for describing quantum dynamics in systems containing quantum field of various nature. At the derivation of the equations of motion, the vibrational part of the wavefunction is expanded over the time-dependent basis of coherent states (Davydov Ansatz [47]), parametrised by the complex-valued eigenvalue $\sigma_\mathbf{k}$ of the corresponding phonon operator: $\hat{b}_\mathbf{k} |\sigma_\mathbf{k}\rangle = \sigma_\mathbf{k} |\sigma_\mathbf{k}\rangle$. Neglecting the higher-order powers of $\hat{B}_\mathbf{q}^\dagger$, the multi-exciton wave-function is chosen in the form (bold σ stands for the set of all $\sigma_\mathbf{k}$ and $|0_\mathbf{q}\rangle$ is the zero \mathbf{q} -exciton state) b

$$|\Psi(t)\rangle = \prod_{\mathbf{q}} \left(G_\mathbf{q}(t) + C_\mathbf{q}(t) \hat{B}_\mathbf{q}^\dagger \right) |0_\mathbf{q}\rangle |\sigma(t)\rangle. \quad (2)$$

Variation of the Schrödinger equation and equating of the independent variations to zero generates coupled equations of motion [44, 46, 48]: equation of a

dumped classical oscillator driven by the excitonic field for $\sigma_{\mathbf{k}}$ and the coupled non-linear extended Schrödinger equation [49] for the expansion coefficients $G_{\mathbf{q}}(t)$ and $C_{\mathbf{q}}(t)$ with the non-linear terms amplitudes proportional to $\sigma_{\mathbf{k}}$. It is convenient to formulate the equations in terms of the complex-valued polarization $Q_{\mathbf{q}} \equiv G_{\mathbf{q}}^* C_{\mathbf{q}} = \langle \Psi | \hat{B}_{\mathbf{q}} | \Psi \rangle$ and the relative population $J_{\mathbf{q}} = \langle \Psi | \hat{J}_{\mathbf{q}} | \Psi \rangle \equiv \langle \Psi | [\hat{B}_{\mathbf{q}}, \hat{B}_{\mathbf{q}}^\dagger] | \Psi \rangle = |G_{\mathbf{q}}|^2 - |C_{\mathbf{q}}|^2$ (t -dependence is assumed). Due to the wavefunction normalizing condition, $|G_{\mathbf{q}}|^2 + |C_{\mathbf{q}}|^2 = 1$ the population $J_{\mathbf{q}}$ ranges from -1 to 1 . For the subsystem of two states and a single LLPM the equations of motion read

$$\dot{\sigma}_{\pm} = -i\omega_{ph}\sigma_{\pm} - \gamma\sigma_{\pm} - i \left\{ \begin{array}{l} D^*[Q_a^*Q_b + Q_d^*Q_c] \\ D[Q_b^*Q_a + Q_c^*Q_d] \end{array} \right\}; \quad (3)$$

$$\dot{J}_a = -4\text{Im} \{ \alpha^* Q_a^* Q_b \}; \quad (4)$$

$$\dot{Q}_a = -iW_a Q_a - iJ_a \alpha^* Q_b, \quad (5)$$

where the dot symbol denotes time-derivative, $\sigma_{\pm} \equiv \sigma_{\pm\mathbf{k}_0}$, $\alpha = D(\sigma_-^* + \sigma_+)$, and $D \equiv D(\mathbf{k}_0)v_0$, where v_0 is the volume of averaging in momentum space. Here and below we use the convention that index $i = a, b, c, d$ replaces \mathbf{q}_i . Equations for the state b are obtained by the replacements $a \leftrightarrow b$ and $\alpha^* \rightarrow \alpha$ in eqs. (4, 5). For d and c states the replacement is $a \rightarrow c$, and $b \rightarrow d$. The dumping term $-\gamma\sigma_{\pm}$ in eq. (3) accounts for energy dissipation into the thermal bath.

The stable stationary solutions STE' and bi-STE'. To consider the case of a single STE' we set $Q_c = Q_d = 0$ and $J_c = J_d = 1$ (fig. 1c). The long-time steady state solution for the phonon amplitudes σ_{\pm} reaches the steady state regime at the phase-locking condition, i.e. when the product $Q_a^* Q_b$ is constant or, at least, slowly changes in time. Then the steady state phonon amplitudes (eq. 3) are $\sigma_{\pm}^{(st.)} = -\frac{D^*}{\omega_{ph} - i\gamma} Q_a^* Q_b$, which generates the typical in STE theory energy scale ω_0 entering the vibration strength $\alpha^{(st)} = -2\omega_0 Q_a^* Q_b$, $\omega_0 \equiv \frac{\omega_{ph}|D|^2}{\omega_{ph}^2 + \gamma^2}$. The semiclassical energy functional is read off directly from the Hamiltonian (eq. 1) by the replacement $\hat{B}_i \rightarrow Q_i$ and $\hat{b}_{\pm\mathbf{k}_0} \rightarrow \sigma_{\pm}$. It plays a role of Lyapunov function, i.e. its minimum corresponds to the stable solution of the equations of motion (eqs. 3, 4, 5). For the stationary regime ($\sigma_{\pm} \rightarrow \sigma_{\pm}^{(st.)}$) under the conservation of the number of excitations condition ($J_a = -J_b$) the functional is a function of a single variable J_a ,

$$H^{(1;a,b)}[J_a] = \bar{W}_{ab} + \frac{\omega_0}{2} \kappa_{ba} J_a - \frac{\omega_0}{8} (1 - J_a^2)^2, \quad (6)$$

where $\bar{W}_{ab} \equiv \frac{W_a + W_b}{2}$ is the mean energy and $\kappa_{ba} \equiv \frac{W_b - W_a}{\omega_0}$. The function $H^{(1)}$ has three special points. Two of them correspond to free excitons: $H^{(1)} \rightarrow W_{a/b}$ at $J_a = \mp 1$. The energy minimum is realised at $J_{a,0} = -J_{b,0} = \kappa_{ba}(1 + \kappa_{ba}^2) + \mathcal{O}(\kappa_{ba}^5)$ with the energy $H_0^{(1)} = \bar{W}_{ab} + \frac{\omega_0}{2} \kappa_{ba} J_{a,0} - 2\eta_{ab}$, and the coupling energy shift $\eta_{ab} = \frac{\omega_0}{16}(1 - J_{a,0}^2)^2$. The minimum exists in a narrow range $|\kappa_{ba}| < 2/\sqrt{27} \sim 0.38$. Therefore, at a fixed

κ_{ba} the STE' particle is stable and coexists with the free excitons (fig. 2a). The effective activation barrier (difference between the maximal and the minimal energies) between this two states is $\frac{\omega_0}{8}(1 - 4|\kappa_{ba}| + 3\kappa_{ba}^2 + \mathcal{O}(\kappa_{ba}^3))$ and becomes negligible on the edges $|\kappa_{ba}| \simeq 0.38$.

To address the regime of high concentrations of excitations we turn our attention to the multiparticle model: two excitons with yet arbitrary energies are entangled with one and the same LLPM. Accounting of the quantum states c and d generates an additional term in the expression for the stationary vibration strength: $\alpha^{(st.)} = -2\omega_0(Q_a^* Q_b + Q_d^* Q_c)$. The conservation of excitations reflected in the relations $J_a = -J_b$ and $J_c = -J_d$ allows to write the semiclassical energy as a function of J_a, J_c and the phase $\Delta = \phi_a - \phi_b + \phi_c - \phi_d$ (where ϕ_i is the time-dependent phase of Q_i):

$$H^{(2)}[J_a, J_c] = H^{(1;a,b)}[J_a] + H^{(1;c,d)}[J_c] - \frac{\omega_0}{4}(1 - J_a^2)(1 - J_c^2) \cos[\Delta(J_a, J_c)]. \quad (7)$$

For the unlocked phase Δ , the last term in eq. (7) oscillates fast. Due to self-averaging, the energy effectively splits into two STE' contributions, which must be minimized independently. In the phase-locked regime, i.e. when Δ reaches the stationary value $\Delta = 0$, the energy $H^{(2)}$ has to be minimized subject to the dynamically generated condition $|\cos[\Delta(J_a, J_c)]| = 1$ (fig. 2b). The energy reaches minimum $H_0^{(2)} = H^{(1;a,b)}[J_{a,1}] + H^{(1;d,c)}[J_{c,1}] - \frac{\omega_0}{4}(1 - J_{a,1}^2)(1 - J_{c,1}^2)$ at the point $J_{a,1} = -J_{b,1} \approx \kappa_{ba}/2$ and $J_{c,1} = -J_{d,1} \approx \kappa_{dc}/2$. The minimal energy phase-locked stationary solution we interpret as bi-STE'. Its energy is always lower than the sum of two STE' energies.

III. ESTIMATION OF THE FLUORESCENT SPECTRA.

By means of the standard technique [24, 50] we calculated the STE' frequency-resolved stationary fluorescent spectrum, with the initial density matrix entries taken from the stationary solution, $C_i = \sqrt{\frac{1 - J_{i,0}}{2}} e^{-i\frac{W_i}{2}t - tH_0^{(1)}}$ and $Q_i = \sqrt{\frac{1 - J_{i,0}^2}{2}} e^{-i\bar{W}_{ab}t}$. The light-matter interaction term in eq. (1) was taken in the rotation-wave approximation, $\hat{\mathcal{H}}' = \sum \Omega_{\mathbf{k}} \hat{a}_{\mathbf{k}}^\dagger \hat{a}_{\mathbf{k}} + iT \sum_{\mathbf{k}} (\hat{B}_{\mathbf{k}} \hat{a}_{\mathbf{k}}^\dagger - \hat{B}_{\mathbf{k}}^\dagger \hat{a}_{\mathbf{k}})$. The natural decay rate into the mode Ω_i is $\beta_i = T^2 \beta / [(\Omega_i - W_i/2 - H_0^{(1)}/2)^2 + \beta^2]$, where $\beta \sim k_B T$ is the temperature-dependent decoherence rate. The fluorescent spectrum of a single STE' $S(\omega) \propto \omega A(\omega - H_0^{(1)}; \kappa_{ba}) \delta(\omega - \Omega_a)$, where $A(\omega - H_0^{(1)}; \kappa_{ba})$ is Gaussian amplitude (resulting from averaging over the vibration modes) with the standard deviation of order $|\tilde{D}| \equiv |D|(1 - J_{a,0}^2) \sqrt{\frac{1}{8} + \frac{\gamma\beta}{4\omega_{ph}^2}}$ and the prefactor $2\sqrt{\pi} T^2 \frac{1 + J_{a,0}}{1 - J_{a,0}} / |\tilde{D}|$. The obtained single-STE' spectrum was averaged over all possible directions of the

vector \mathbf{k}_0 . Technically, this procedure translates into averaging over κ_{ba} within the permitted limits. After the averaging the central peak shifts towards the arithmetic mean of the highest and the lowest single-STE' frequencies (fig. 2c). For the large phonon-exciton interactions, $|D| \sim \omega_0$, the fluorescent peak position can be approximated by $\approx W_a - 0.22\omega_0$.

For the case of mirror-symmetric bi-STE' (Fig. 1e), when $W_a = W_c$ and $W_b = W_d$, $\mathbf{q}_a = -\mathbf{q}_c$ and $\mathbf{q}_b = -\mathbf{q}_d$, the wavefunction expansion coefficients are $C_a = C_c = \sqrt{\frac{1-J_{a,1}}{2}}e^{-i\frac{W_a}{2}t - i\frac{1}{4}H_0^{(2)}t}$, $C_b = C_d = \sqrt{\frac{1+J_{a,1}}{2}}e^{-i\frac{W_b}{2}t - i\frac{1}{4}H_0^{(2)}t}$, and $Q_i = \frac{\sqrt{1-J_{a,1}}}{2}e^{-i\bar{W}_{ab}t}$. The Hamiltonian of the mirror-symmetric bi-STE' can be recast in the form of the Dicke Hamiltonian ($\hat{B} = \hat{B}_a + \hat{B}_c$, $\hat{J} = \hat{J}_a + \hat{J}_c$)

$$\tilde{\mathcal{H}} = \frac{H_0^{(2)}}{2}\hat{J} + \Omega_a\hat{a}_1^\dagger\hat{a}_1 - i\frac{T}{\sqrt{2}}\left[\hat{B}^\dagger\hat{a}_1 - \hat{B}\hat{a}_1^\dagger\right], \quad (8)$$

and the same Hamiltonian for b and d . The approximate Hamiltonian (eq. 8) follows from the Heisenberg equations written for the steady-state regime when the negligibly small odd combinations, like $\hat{B}_a - \hat{B}_c$, are omitted. In the bi-STE' decay process the light irradiates anisotropically into the mode $\hat{a}_1 = (\hat{a}_{\mathbf{q}_a} + \hat{a}_{-\mathbf{q}_a})/\sqrt{2}$.

The Hamiltonian (eq. 8) commutes with the parity operator $\hat{a}_1^\dagger\hat{a}_1 + \hat{J}/2$, so that spontaneous decay of one exciton (spontaneous symmetry breaking) causes immediate decay of the other. This phenomenon is known as superradiance and is characterized by rapid decay, twice faster than the natural one. The time-dependent spectrum [24] $S(\omega, t) \propto \pi T^2 \omega \delta(\omega - H_0^{(2)}/2) \sum_{i=a,b} (1 - J_{i,1}^2) \text{sech}^2 [2\beta_i(t - \gamma^{-1})]$, where γ^{-1} now plays a role of

the bi-STE' formation characteristic time. Since the value of κ_{ba} in the bi-STE' is fixed, the averaging over \mathbf{k}_0 results in multiplication on the time-dependent concentration of the mirror-symmetric bi-STE, $n_{bi}(t)$. The latter can be described by a system of non-Markovian kinetic equations ($\bar{\beta} = \beta_a + \beta_b$)

$$\dot{n}_{bi} = f_1 n_{ex}^2 (1 - e^{-\gamma t}) - f_2 n_{bi} - \bar{\beta} n_{bi}; \quad (9)$$

$$\dot{n}_{ex} = -f_1 n_{ex}^2 + f_2 n_{bi}. \quad (10)$$

Starting from some non-zero concentrations of excitons $n_{ex}(0) = n_0$ and $n_{bi}(0) = 0$, the concentration $n_{bi}(t)$ increases quadratically with time (see the insert in fig. 2c) reaches the maximal height, which is proportional to n_0^2 , and decays following the inverse quadratic law. The found time behaviour agrees with the experimental observations [15].

Finally, using our model, one can estimate the energetic parameters of the system. Associating the obtained theoretical peaks with their experimental values, we find that $\omega_0 \approx 0.06\text{eV}/(0.43 - 0.22) = 0.28\text{eV}$, so that at $\gamma \sim \omega_{ph}/5$, and $\omega_{ph} = 0.014\text{eV}$ we get $|D| \approx 0.06\text{eV} \approx 4.6\omega_{ph}$, which is larger than $k_B T$ for room temperature $\sim 0.026\text{eV}$. Notice that at the choice $|D| = \omega_0$, the calculated spectrum width is almost twice as large as the experimental one, which, in particular, is explained by the Gaussian approximation of the single-STE' spectra used in the averaging.

A justified assumption of exciton wave-packet strong localization in a thermalised non-linear media was essential for our approach. However, this requires further study, especially regarding possible soliton solutions [35]. Further extension of the theory to the time-dependent κ case would make it a general dynamic theory of high-energy-exciton \rightarrow STE \rightarrow low-energy-exciton transition.

-
- [1] D. Emin, *Polarons*. Cambridge University Press, 2012.
- [2] J. T. Devreese and A. S. Alexandrov, "Fröhlich polaron and bipolaron: recent developments," *Reports on Progress in Physics*, vol. 72, no. 6, p. 066501, may 2009. [Online]. Available: <https://dx.doi.org/10.1088/0034-4885/72/6/066501>
- [3] P. P. Schmidt, "The interaction between mott-wannier excitons in a vibrating lattice," *J. Phys. C: Solid State Phys.*, vol. 2, pp. 785–795, 1969.
- [4] R. T. Williams and K. S. Song, "The self-trapped exciton," *Journal of Physics and Chemistry of Solids*, vol. 51, pp. 679–716, 1990. [Online]. Available: <https://api.semanticscholar.org/CorpusID:96726841>
- [5] F. Jiang, Z. Wu, M. Lu, Y. Gao, X. Li, X. Bai, Y. Ji, and Y. Zhang, "Broadband emission origin in metal halide perovskites: Are self-trapped excitons or ions?" *Advanced Materials*, vol. 35, no. 51, p. 2211088.
- [6] J. Tan, D. Li, J. Zhu, N. Han, Y. Gong, and Y. Zhang, "Self-trapped excitons in soft semiconductors," *Nanoscale*, vol. 14, pp. 16394–16414, 2022. [Online]. Available: <http://dx.doi.org/10.1039/D2NR03935D>
- [7] M. Ueta, H. Kanzaki, K. Kobayashi, Y. Toyozawa, and E. Hanamura, *Excitons in Condensed Rare Gases*. Berlin, Heidelberg: Springer Berlin Heidelberg, 1986, pp. 285–308.
- [8] K.-i. Mizuno and A. Matsui, "Frenkel exciton dynamics in anthracene under high pressure and quasi-free exciton state," *Journal of the Physical Society of Japan*, vol. 55, no. 7, pp. 2427–2435, 1986. [Online]. Available: <https://doi.org/10.1143/JPSJ.55.2427>
- [9] J. Singh and A. Matsui, "Free, quasifree, momentarily trapped, and self-trapped exciton states in molecular crystals," *Phys. Rev. B*, vol. 36, pp. 6094–6098, Oct 1987. [Online]. Available: <https://link.aps.org/doi/10.1103/PhysRevB.36.6094>
- [10] T. Hayashi, T. Kobayashi, M. Iwanaga, and M. Watanabe, "Exciton dynamics related with phase transitions in cspbcl3 single crystals," *Journal of Luminescence*, vol. 94-95, pp. 255–259, 2001, international Conference on Dynamical Processes in Excited States of Solids. [Online]. Available: <https://www.sciencedirect.com/science/article/pii/S0022231301002897>

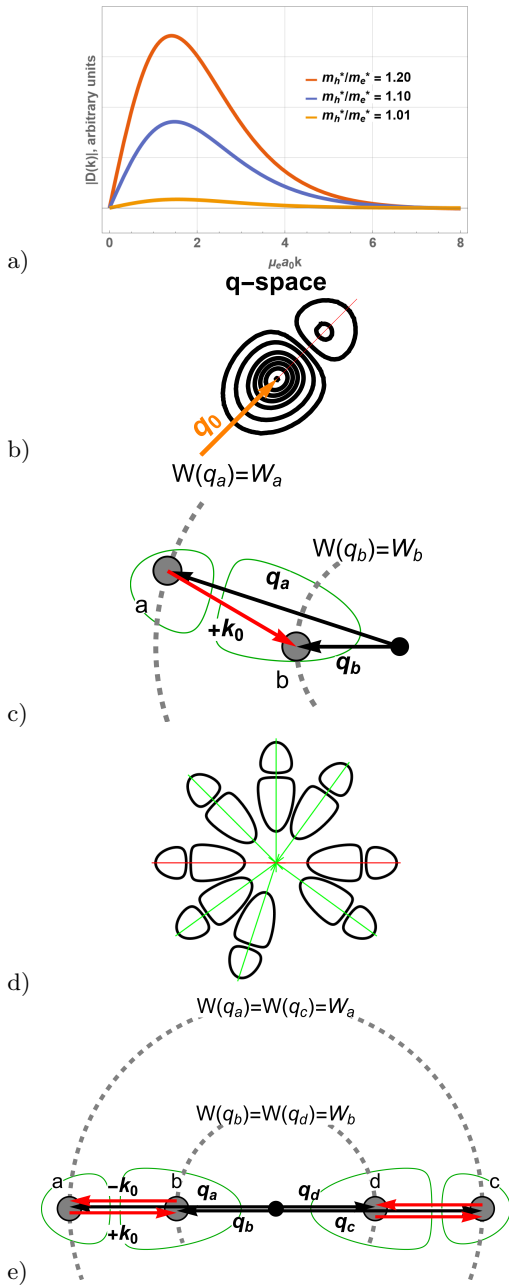


FIG. 1. (a) The Frölich exciton-phonon interaction amplitude plotted vs. the dimensionless wavevector $\mu_e a_0 k$, where a_0 is the exciton Bohr radius, and μ_e is the ratio of the electron effective mass and the exciton reduced mass, $\mu_e = m_h^*/(m_e^* + m_h^*)$. The position of maximum is at the point $\mu_e a_0 k \sim 2$ and almost independent on the ratio m_h^*/m_e^* . (b) In the momentum space the wave packet is described by heavy-tail distribution due to thermal and non-linear localisation in the coordinate space, and the LLPM vector \mathbf{k}_0 can fit inside the packet at least once. (c) In our model the whole exciton wave packet is replaced by two quantum states a and b (with energies W_a and W_b , respectively) connected by the vector \mathbf{k}_0 . The STE' state is reached when the phonon modes become entangled with exciton wave packet. The vectors \mathbf{q}_a and \mathbf{q}_b are not necessary collinear to \mathbf{k}_0 , such detuning results in the angular motion of STE' shifting it to the configuration with the maximal difference between W_a and W_b . (d) At high concentrations of excitations due to effective repulsion, the packets can form the mirror-symmetric configurations (along red line in the figure), which are the source of superfluorescence. (e) The mirror-symmetric bi-STE' is composed of two excitons entangled with one and the same LLPM.

- [11] A. Dey, J. Ye, A. De, E. Debroye, S. K. Ha, E. Bladt, A. S. Kshirsagar, Z. Wang, J. Yin, Y. Wang, L. N. Quan, F. Yan, M. Gao, X. Li, J. Shamsi, T. Debnath, M. Cao, M. A. Scheel, S. Kumar, J. A. Steele, M. Gerhard, L. Chouhan, K. Xu, X.-g. Wu, Y. Li, Y. Zhang, A. Dutta, C. Han, I. Vincon, A. L. Rogach, A. Nag, A. Samanta, B. A. Korgel, C.-J. Shih, D. R. Gamelin, D. H. Son, H. Zeng, H. Zhong, H. Sun, H. V. Demir, I. G. Scheblykin, I. Mora-Seró, J. K. Stolarczyk, J. Z. Zhang, J. Feldmann, J. Hofkens, J. M. Luther, J. Pérez-Prieto, L. Li, L. Manna, M. I. Bodnarchuk, M. V. Kovalenko, M. B. J. Roeffaers, N. Pradhan, O. F. Mohammed, O. M. Bakr, P. Yang, P. Müller-Buschbaum, P. V. Kamat, Q. Bao, Q. Zhang, R. Krahne, R. E. Galian, S. D. Stranks, S. Bals, V. Biju, W. A. Tisdale, Y. Yan, R. L. Z. Hoyer, and L. Polavarapu, "State of the art and prospects for halide perovskite nanocrystals," *ACS Nano*, vol. 15, no. 7, pp. 10775–10981, 2021, pMID: 34137264. [Online]. Available: <https://doi.org/10.1021/acsnano.0c08903>
- [12] Y. Yu, C. Zhao, L. Ma, L. Yan, B. Jiao, J. Li, J. Xi, J. Si, Y. Li, Y. Xu, H. Dong, J. Dai, F. Yuan, P. Zhu, A. K.-Y. Jen, and Z. Wu, "Harvesting the triplet excitons of quasi-two-dimensional perovskite toward highly efficient white light-emitting diodes," *The Journal of Physical Chemistry Letters*, vol. 13, no. 16, pp. 3674–3681, 2022, pMID: 35438498. [Online]. Available: <https://doi.org/10.1021/acs.jpclett.2c00996>
- [13] R. Bonifacio and L. A. Lugiato, "Cooperative radiation processes in two-level systems: Superfluorescence," *Phys. Rev. A*, vol. 11, pp. 1507–1521, May 1975. [Online]. Available: <https://link.aps.org/doi/10.1103/PhysRevA.11.1507>
- [14] G. Findik, M. Biliroglu, D. Seyitliyev, J. Mendes, A. Barrette, H. Ardekani, L. Lei, Q. Dong, F. So, and K. Gundogdu, "High-temperature superfluorescence in methyl ammonium lead iodide," *Nature Photonics*, vol. 15, no. 9, pp. 676 – 680, 2021. [Online]. Available: <https://doi.org/10.1038/s41566-021-00830-x>
- [15] M. Biliroglu, G. Findik, J. Mendes, D. Seyitliyev, L. Lei, Q. Dong, Y. Mehta, V. V. Temnov, F. So, and K. Gundogdu, "Room-temperature superfluorescence in hybrid perovskites and its origins," *Nature Photonics*, vol. 16, pp. 324–329, 2022.
- [16] J. Tilchin, D. N. Dirin, G. I. Maikov, A. Sashchiuk, M. V. Kovalenko, and E. Lifshitz, "Hydrogen-like wigner-mott excitons in single crystal of methylammonium lead bromide perovskite," *ACS Nano*, vol. 10, no. 6, pp. 6363–6371, 2016, pMID: 27249335. [Online]. Available: <https://doi.org/10.1021/acsnano.6b02734>
- [17] D. Zhao, J. M. Skelton, H. Hu, C. La-o vorakiat, J.-X. Zhu, R. A. Marcus, M.-E. Michel-Beyerle, Y. M. Lam, A. Walsh, and E. E. M. Chia, "Low-frequency optical phonon modes and carrier mobility in the halide perovskite CH₃NH₃PbBr₃ using terahertz time-domain spectroscopy," *Applied Physics Letters*, vol. 111, no. 20, p. 201903, 11 2017. [Online]. Available: <https://doi.org/10.1063/1.4993524>
- [18] M. Nagai, T. Tomioka, M. Ashida, M. Hoyano, R. Akashi, Y. Yamada, T. Aharen, and Y. Kanemitsu, "Longitudinal optical phonons modified by organic molecular cation motions in organic-inorganic hybrid perovskites," *Phys. Rev. Lett.*, vol. 121, p. 145506, Oct 2018. [Online]. Available: <https://link.aps.org/doi/10.1103/PhysRevLett.121.145506>

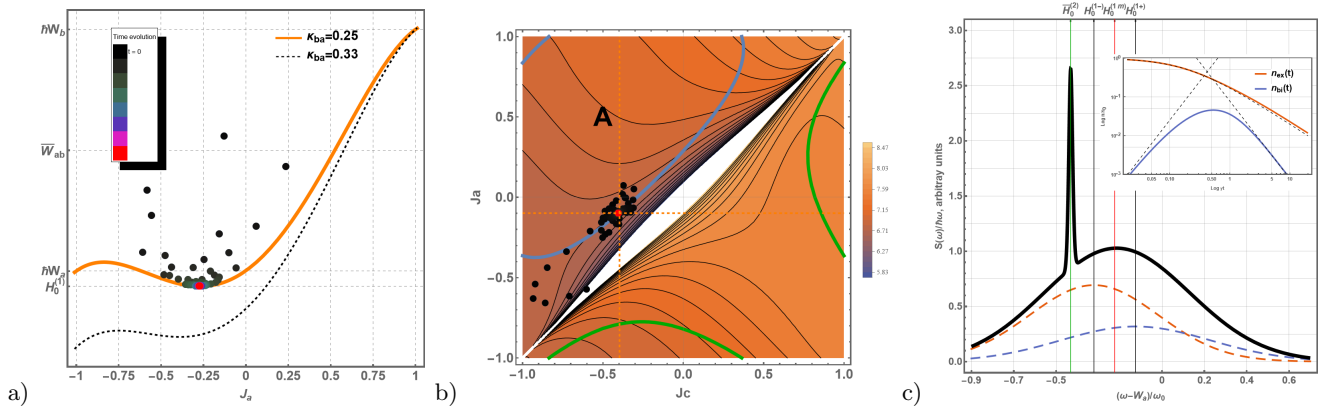


FIG. 2. (a) The semiclassical stationary energy $H^{(1)}$ (orange curve, eq. 6) and numeric solution (coloured dots) of the equations of motion (eqs. 3, 4, 5, fig. 1c) at $\kappa = 0.25$. The dots show the energy and the relative population J_a of the exciton-phonon subsystem during its evolution. Colours depict the time step: from black at small times to red at larger times. The system evolves from some non-stationary high-energy state towards the stationary solution corresponding to the energy minimum. The function $H^{(1)}$ plotted at $\kappa_{ba} = -0.33$ (dashed black) is given for comparison. (b) The semiclassical stationary energy for the bi-STE' $H^{(2)}$ (eq. 7) plotted as a function of the occupations J_a , and J_c at $\kappa_{ba} = 0.18$, and $\kappa_{dc} = 0.74$ (see scheme in fig. 1e but with non-equal energies $W_a \neq W_c$, and $W_b \neq W_d$) and numeric solution of the equations of motion (the dots' colours were chosen as in fig.a). In the region "A" surrounded by blue solid curve $0 < \cos \Delta \leq 1$, while in the regions surrounded by green curves $-1 \leq \cos \Delta < 0$. The stationary state solution corresponds to the energy minimum at the blue curve, where $\cos \Delta = 1$. (c) The averaged over \mathbf{k}_0 directions (over κ_{ba}) STE' spectrum (black curve) plotted vs frequency ω measured in units ω_0 , at $|D| = \omega_0$. For comparison the spectra of single-STE' are plotted for the largest $\kappa_{ba} = 0.33$ (orange dashed) and the smallest $\kappa_{ba} = 0$ (blue dashed). The maxima are positioned at $H_0^{(1\pm)} = \left(H_0^{(1)}/\omega_0 - W_a/\omega_0 \right) \Big|_{\kappa_{ba} = -0.33, 0}$, and their mean value is denoted by $H_0^{(1m)} = (H_0^{(1+)} + H_0^{(1-)})/2 \approx -0.22$. The superfluorescent (δ -)peak is positioned at $\tilde{H}_0^{(2)} = H_0^{(2)}/\omega_0 \Big|_{\kappa_{ba} = -0.33} \sim -0.43$. In the insert: the typical solution of the system of kinetic equations (eqs. 9, 10) for the superfluorescent peak intensity. The dashed lines shows the asymptotic: $n_{bi}(t) \sim f_1 \gamma n_0^2 t^2 / 2$, $n_{bi}(t) \sim f_1^{-1} t^{-2} (\tilde{\beta} + f_2) / \tilde{\beta}^2$, $n_{ex}(t) \sim n_0 / (1 + f_1 n_0 t)$, the maximum is reached at $t_0 \sim \sqrt[4]{2(\tilde{\beta} + f_2) / f_1^2 \gamma \tilde{\beta}^2 n_0^2}$ and the maximal height is $\sim n_0^2 f_1 \gamma t_0 / (f_2 + \tilde{\beta})(1 + f_1 n_0 t_0)^2$.

1103/PhysRevLett.121.145506

- [19] M. Sendner, P. K. Nayak, D. A. Egger, S. Beck, C. Müller, B. Epping, W. Kowalsky, L. Kronik, H. J. Snaith, A. Pucci, and R. Lovrinčić, "Optical phonons in methylammonium lead halide perovskites and implications for charge transport," *Mater. Horiz.*, vol. 3, pp. 613–620, 2016. [Online]. Available: <http://dx.doi.org/10.1039/C6MH00275G>
- [20] A. D. Wright, C. Verdi, R. L. Milot, G. E. Eperon, M. A. Pérez-Osorio, H. J. Snaith, F. Giustino, M. B. Johnston, and L. M. Herz, "Electron-phonon coupling in hybrid lead halide perovskites," vol. 7, p. 11755, 2016. [Online]. Available: <https://doi.org/10.1038/ncomms11755>
- [21] Y. Yamada and Y. Kanemitsu, "Electron-phonon interactions in halide perovskites," *NPG Asia Materials*, vol. 14, p. 48, 2022. [Online]. Available: <https://doi.org/10.1038/s41427-022-00394-4>
- [22] S. Adachi, "Gaas, alas, and al_xga_{1-x}as: Material parameters for use in research and device applications," *Journal of Applied Physics*, vol. 58, no. 3, pp. R1–R29, 08 1985.
- [23] D. Seyitliyev, X. Qin, M. K. Jana, S. M. Janke, X. Zhong, W. You, D. B. Mitzi, V. Blum, and K. Gundogdu, "Coherent phonon-induced modulation of charge transfer in 2d hybrid perovskites," *Advanced Functional Materials*, vol. 33, no. 21, p. 2213021, 2023. [Online]. Available: <https://onlinelibrary.wiley.com/doi/abs/10.1002/adfm.202213021>
- [24] C. Leonardi, F. Persico, and G. Vetri, "Dicke model and the theory of driven and spontaneous emission," *La Rivista del Nuovo Cimento (1978-1999)*, vol. 9, pp. 1–85, 1986. [Online]. Available: <https://api.semanticscholar.org/CorpusID:120444837>
- [25] A. V. Andreev, V. I. Emel'yanov, and Y. A. Il'inskii, "Collective spontaneous emission (dicke superradiance)," *Physics-Uspekhi*, vol. 23, pp. 493–514, 1980. [Online]. Available: <https://api.semanticscholar.org/CorpusID:122020443>
- [26] I. Protsenko and A. Uskov, "Superradiance of several atoms near a metal nanosphere," *Quantum Electronics*, vol. 45, no. 6, p. 561, jun 2015. [Online]. Available: <https://dx.doi.org/10.1070/QE2015v045n06ABEH015675>
- [27] T. Meier, Y. Zhao, V. Chernyak, and S. Mukamel, "Polarons, localization, and excitonic coherence in superradiance of biological antenna complexes," *The Journal of Chemical Physics*, vol. 107, no. 10, pp. 3876–3893, 09 1997. [Online]. Available: <https://doi.org/10.1063/1.474746>
- [28] H. Fröhlich, "Electrons in lattice fields," *Advances in Physics*, vol. 3, no. 11, pp. 325–361, 1954. [Online]. Available: <https://doi.org/10.1080/00018735400101213>
- [29] J. Singh, *Excitation Energy Transfer Processes in Condensed Matter*. Boston, MA: Springer, 1994.
- [30] P. Y. Yu and M. Cardona, *Fundamentals of Semiconductors*. Springer Berlin, 2016.
- [31] B. D. Fainberg and V. A. Osipov, "Theory of high-temperature superfluorescence in hybrid perovskite

- thin films,” *The Journal of Chemical Physics*, vol. 161, no. 11, p. 114705, 09 2024. [Online]. Available: <https://doi.org/10.1063/5.0226221>
- [32] K. Frohna, T. Deshpande, J. Harter, W. Peng, B. Barker, J. Neaton, S. Louie, O. Bakr, D. Hsieh, and M. Bernardi, “Inversion symmetry and bulk rashba effect in methylammonium lead iodide perovskite single crystals,” *Nature Communications*, vol. 9, p. 1829, 2018. [Online]. Available: <https://doi.org/10.1038/s41467-018-04212-w>
- [33] C.-P. Sun and L.-H. Yu, “Exact dynamics of a quantum dissipative system in a constant external field,” *Phys. Rev. A*, vol. 51, pp. 1845–1853, Mar 1995. [Online]. Available: <https://link.aps.org/doi/10.1103/PhysRevA.51.1845>
- [34] D. Schuch, K.-M. Chung, and H. Hartmann, “Nonlinear schrödinger-type field equation for the description of dissipative systems. i. derivation of the nonlinear field equation and one-dimensional example,” *Journal of Mathematical Physics*, vol. 24, pp. 1652–1660, 1983. [Online]. Available: <https://api.semanticscholar.org/CorpusID:120005353>
- [35] B. A. Malomed, “Index,” in *Multidimensional Solitons*. AIP Publishing LLC. [Online]. Available: <https://doi.org/10.1063/9780735425118.index>
- [36] X. Zang, S. Montangero, L. D. Carr, and M. T. Lusk, “Engineering and manipulating exciton wave packets,” *Phys. Rev. B*, vol. 95, p. 195423, May 2017. [Online]. Available: <https://link.aps.org/doi/10.1103/PhysRevB.95.195423>
- [37] D. Schuch, K.-M. Chung, and H. Hartmann, “Nonlinear schrödinger-type field equation for the description of dissipative systems. iii. frictionally damped free motion as an example for an aperiodic motion,” *Journal of Mathematical Physics*, vol. 25, no. 10, pp. 3086–3092, 10 1984. [Online]. Available: <https://doi.org/10.1063/1.526024>
- [38] V. E. Zakharov and A. B. Shabat, “Exact theory of two-dimensional self-focusing and one-dimensional self-modulation of waves in nonlinear media,” *Journal of Experimental and Theoretical Physics*, vol. 34, pp. 62–69, 1970.
- [39] M. Combescot, O. Betbeder-Matibet, and F. Dubin, “Mixture of composite-boson molecules and the pauli exclusion principle,” *Phys. Rev. A*, vol. 76, p. 033601, Sep 2007. [Online]. Available: <https://link.aps.org/doi/10.1103/PhysRevA.76.033601>
- [40] H. Haken, “On the quantum theory of the multi-electron system in the oscillating lattice. i,” *Z. Phys.*, vol. 146, pp. 527–554, 1956, [in German].
- [41] R. J. Elliott, “Intensity of optical absorption by excitons,” *Phys. Rev.*, vol. 108, pp. 1384–1389, Dec 1957. [Online]. Available: <https://link.aps.org/doi/10.1103/PhysRev.108.1384>
- [42] A. Miyata, A. Mitoglu, P. Plochocka, O. Portugall, J.-W. Wang, S. Stranks, H. Snaith, and R. Nicholas, “Direct measurement of the exciton binding energy and effective masses for charge carriers in organic–inorganic tri-halide perovskites,” *Nature Physics*, vol. 11, p. 582, 2015. [Online]. Available: <https://doi.org/10.1038/nphys3357>
- [43] G. Antonius and S. G. Louie, “Theory of exciton-phonon coupling,” *Phys. Rev. B*, vol. 105, p. 085111, Feb 2022. [Online]. Available: <https://link.aps.org/doi/10.1103/PhysRevB.105.085111>
- [44] W. H. Miller, “On the relation between the semiclassical initial value representation and an exact quantum expansion in time-dependent coherent states,” *The Journal of Physical Chemistry B*, vol. 106, no. 33, pp. 8132–8135, 2002. [Online]. Available: <https://doi.org/10.1021/jp020500>
- [45] V. Osipov and B. Fainberg, “Hartree method for molecular polaritons,” *Phys. Rev. B*, vol. 107, p. 075404, 2023.
- [46] H.-D. Meyer, U. Manthe, and L. Cederbaum, “The multi-configurational time-dependent hartree approach,” *Chemical Physics Letters*, vol. 165, no. 1, pp. 73–78, 1990. [Online]. Available: <https://www.sciencedirect.com/science/article/pii/0009261490870141>
- [47] A. S. Davydov and N. I. Kislukha, “Solitary excitons in one-dimensional molecular chains,” *physica status solidi (b)*, vol. 59, no. 2, pp. 465–470, 1973. [Online]. Available: <https://onlinelibrary.wiley.com/doi/abs/10.1002/pssb.2220590212>
- [48] E. Artacho and D. O’Regan, “Quantum mechanics in an evolving hilbert space,” *Physical Review B*, vol. 95, p. 115155, 2017. [Online]. Available: <https://doi.org/10.1103/PhysRevB.95.115155>
- [49] N. A. B. Aklan, N. A. S. Ishak, and B. A. Umarov, “Vector soliton in coupled nonlinear schrödinger equation,” *Journal of Physics: Conference Series*, vol. 1988, no. 1, p. 012015, jul 2021. [Online]. Available: <https://dx.doi.org/10.1088/1742-6596/1988/1/012015>
- [50] M. Scully and M. Zubairy, *Quantum Optics*, ser. Quantum Optics. Cambridge University Press, 1997.